



10-1-11

DYNAMIC EXPERIMENTS AND NUMERICAL SIMULATIONS OF MODEL CONCRETE-FACE ROCKFILL DAMS

Guocheng HAN, Xianjing KONG and Junjie LI

Department of Civil Engineering, Dalian University
of Technology, Dalian, China

SUMMARY

In this paper, the dynamic response characteristics and failure phenomena of two kinds of model dams, i.e., homogeneous rockfill dams and faced rockfill dams, are investigated by large scale shaking table tests; abundant numerical simulations of model dams are performed by the finite element method considering the nonlinearity of materials; and the results are compared with those from the corresponding dynamic experiments.

INTRODUCTION

In the last two decades, concrete-faced rockfill dams (CFRD) are more and more acknowledged as a new dam type with its widespread developing prospects as pointed out by Cook, et al. (1985). As this type of dam possesses many favoured aspects, such as the lowest cost, easy construction and reliable operation, the CFRD is rapidly developing in China. Unfortunately, the current design and construction of the CFRD mainly depend on the experience achieved from the constructed projects in the world. Obviously, a deeper rational knowledge about the states of stress, the deformation characteristics and the stability of the facing slab, especially dynamic responses and failure phenomena of the CFRD under seismic loading, are not available.

The existent CFRDs were mostly built in the low or moderate seismically active areas, and their running periods were also not long. It is not certain whether their experience can directly adapt to the CFRD in strong seismic areas, the further research is urgently required. In this paper, we regard the model dams as the object of studies, and conduct a series of resonance and failure experiments for two kinds of model dams, i.e., homogeneous rockfill dams and faced rockfill dams. Then, the resonant characteristics between two kinds of model dams are compared, and the possible failure phenomena under strong earthquakes as well as the effects of several related factors are systematically studied. Finally, a computer program using the finite element method is worked out. Based on the comparison of the experimental results with the numerical simulations, some new understanding about the dynamic behavior of the CFRD has been gained.

GENERAL DESCRIPTION OF MODEL EXPERIMENTS

The seismic-simulation shaking table used in the studies has a size of 3x3 m. The model dams are constructed in a steel container(4x1x1 m) with a plexiglass plate only on the vertical face fixed upon the shaking table.

The model dams used for the experiments are 1.0 m high, with a slope gradient of 1:1.4 both in the upstream and in the downstream. For the model faced rockfill dams, the thickness of slab is 4 mm, and the filter under the slab is 2.5 cm thick. Twelve accelerometers are previously embedded in the dam bodies, seven strain gauges are posted on the slab surface. The cross section of the model dams used in the experiments is given in Fig.1.

We select the limestone of which the specific gravity is 2.71 as the construction materials of model dams. In Fig.2, A,B respectively represent the gradation curve of the materials for the dam shell and the filter. The compacting is done manually to the required density. All of the model dams are controlled to identical densities(unit weights are 1.59 t/m³ for the dam shell, and 1.71 t/m³ for the filter). The facing slab with a size of 170x100x0.4 cm is poured by a mixed paste consisting of the gypsum and other materials according to a prescribed fitting ratio. The resulting dynamic Young's modulus is approximately 24000-26000 kgf/cm², and the tensile strength is about 1.6-3.0 kgf/cm².

Resonance Experiments In order to get a clear understanding of the influence of the facing slab on the free vibration characteristics of dam body, the first modal shapes and frequencies are measured for both homogeneous and faced rockfill dams. Referring to the difficulty manifested in measurements of higher modes due to limitation of the frequency range of the shaking table, we applied the program SAP-5 to calculate the first six modes. The results of model experiments together with calculations show that the facing slab enhances the overall restraint, the characteristics of faced rockfill dams are somewhat different from homogeneous rockfill dams, even though the slab is extremely thick.

(1) The slight increases of frequencies of model dams due to the facing slab

The measured and computational frequencies are given in Table 1 for three different model rockfill dams. Obviously, the contribution of the facing slabs to the overall stiffness of faced rockfill dams effectively enhances the natural frequencies of the dams, especially for the transverse vibration modes. For example, compared with the homogeneous rockfill dam, frequency increase of transverse modes for two rockfill dams respectively faced with gypsum and plexiglass, having different material modulus E_f , 26000kgf/cm² and 39000kgf/cm², are individually up to about 5-6%, 7-8%.The relative increases η of frequencies versus the ratio between material modulus of the facing slab and the dam are presented in Fig.3, in which f_d , f_{fd} respectively stand for the natural frequencies of the homogeneous dam and the faced dam.

For the practical prototype dam, the average Young's modulus E_d of which is closely related to its height, subsequently, the ratio of E_f/E_d decreases with the height of dam. The lower the dam, the more serious the influence of the slab on the free vibration characteristics of the dam is.

(2) Difference on modal shapes

The comparison for transverse modal shapes is shown in Fig.4, where the continuous lines stand for the homogeneous rockfill dam and the dash lines stand for the faced rockfill dam with the slab being made of the gypsum. There are some suggestions that the bending effect of the dam body is increased to some extent. The modal shapes of both types of dams are slightly different, and their discrepancies tend to increase with the number of mode. This possibly results from the significant difference between the physical properties of the slab and the soil.

(3) The free vibration of the faced rockfill dam with storage of water

Through free vibration tests of eleven model faced rockfill dams with six

different levels of water, it is found that the vibration frequencies with storage of water are nearly identical to those measured without the storage of water and their difference of the modal shapes cannot be recognized too. In fact, the effective stress and the stiffness of the dam body are increased due to dynamic water pressure on the upstream face. On the other hand, owing to the adoption of a flatter slope, the relative weight of the added mass is of minor prominence.

Failure Experiments In the dynamic failure tests, each model dam is excited on the shaking table by applying the sinusoidal base motions, the frequency of which is kept a constant (20 Hz) and the intensity is gradually increased up to the initiation of failure when cracking in the slab occurs.

(1) Description of the failure process

A fact is first confirmed that both model homogeneous and faced rockfill dams have an identical form of the initial failure, that is, the shallow-seated sliding of the slope in the vicinity of the crest and the subsequent subsiding near the crest. As the exciting intensity increases, the quantities of grains participating in sliding gradually increases, resulting in the expansion of the failing zone. Their difference is that the sliding of grains occurs symmetrically on both slope surfaces for the homogenous rockfill dam, and only on the downstream slope surface for the faced rockfill dam. In the latter case, the upstream slope has a rather high stability because of the action of the facing slab.

Based on numerous experimental observations, the failure occurrence and development of model faced rockfill dams can be roughly divided into three stages as following. (a) Initial sliding--when the amplitudes of the ground acceleration increase up to 140 gal, the grains and small gravels on the downstream slope near the crest are inclined to slide downwards. (b) Sliding with flattening of soil mass near the crest--as the intensity increases continuously, in company with massive sliding and rolling of gravels, the soil mass near the crest starts to flatten. In the case of no water or the level of water lower than $2H/3$, where H is the dam height, the materials of the filter have a significant trend to the downward slip with a serious outward bulge in the middle of the slab. (c) Fracture of the slab--the slab becomes a cantilever structure because of the loss of the restrain of soil mass due to sliding and rolling, it can violently vibrate. As the intensity increases, the horizontal cracks occur in the upper portion of the slab, immediately afterwards an eventual fracture is impending. Especially, in the case of no storage of water, a rapid downward slip of the grains of the filter leads to serious bulge on the middle of the slab. The failure states of the model dams are shown in Fig.5.

As previously described, the failure of the faced rockfill dams possesses two obvious features, i.e., the initial slip of the downstream slope surface near the crest and the initial cracks on the upper portion of the facing slab. An important reason causing the eventual fracture of the slab is the failing of soil mass near the crest, such as the loosening, sliding and subsiding of the soil.

(2) The influence of water level on the position of the fracture of slab

Fig.6 portrays the occurrence sequence of the fracture of the slab for three different model dams with three water levels. It appears that the first crack occurs on the upper slab which is independent of the storage of water. Table 2 gives the measured data presenting the position of initial fracture of the slab under the different water levels. The position where the fracture occurs moves up as the water level rises. In addition, after the initial fracture of the slab, the downward movement tendency of the grains makes the slab bulge towards the upstream. In the case of water storage, the water pressure exerted on the slab avoids the slab bulging out, consequently, the cracks easily occur near the water surface where is the intersection among non-balance forces. In the case of the

empty reservoir, because of no water pressure on the slab, the slab is free to bulge towards the upstream, the crack is inclined to occur in the lower position (Fig.6).

The acceleration values(point A-5) measured at the beginning of the fracture of the slab are shown in Fig.7. It seems that the acceleration amplitudes at the position of the fracture of the slab nearly hold a constant, on an average, 0.55g, under the different water levels, and the amplitudes of the input acceleration are inversely proportional to the water levels, that is, the higher the water level is, the more easily the cracks occur on the slab.

NUMERICAL ANALYSIS PROCEDURE

Analytical Model The dynamic numerical analyses of model dam are performed using the computer program QUAD-4(Idriss, et al,1973). In order to consider the structural characteristics of the faced rockfill dams, several treatments are especially made and calculation are carried out with the micro-computer IBM-PC/XT.

(1) Two special elements--(a) As the facing slab is extremely thick but its stiffness cannot be overlooked, the slab is divided into a set of beam elements for the plane problem. (b) The moduli of deformation of the facing slab and rockfill materials are of difference, the slip and separation between boundaries of two media may occur during strong earthquakes. Hence, in the boundaries between the facing slab and the filter material the joint elements are especially constructed(Goodman,1976).

(2) Failure criteria--(a) For the failure of the soil in embankment, the Mohr-Coulomb criterion is utilized in these elements. Two kinds of failure, i.e., the tensile failure, which means that the tensile stress σ_3 exceeds the tensile strength σ_p , and the shear failure, which means that the maximum shear stress τ_{max} exceeds the shear strength τ_y , are taken into consideration(see Fig.8). In the calculations, if the outside elements located in the downstream slope and the crest surface were in the failing state, the shear modulus G of these elements would be given a small value and they do not carry on their functions in the next step. The inside elements associated with the failure elements will be taken as the new outside elements. For the inside failing elements, special modifications on the Mohr circles of their stresses are made as shown in Fig.8. According to the revised maximum shear strains γ_{max} , the shear modulus can be obtained from the $\tau \sim \gamma$ curve. (b) For the sliding and separating of joints between the slab and the embankment, The constitutive relationship of the elements is assumed to be the elastic--completely plastic behaviour (Ref.1). The failure of joint elements can be also classified into two kinds, the sliding and the separating. In the case of the normal strain $\epsilon_n \geq 0$ in the joint elements, the separation failure occurs; when the shear stresses $|\tau|$ in the joint elements exceed the yielding stress $|\tau_y|$ which is defined by the Mohr-Coulomb criterion, the slip failure is initiated. (c) The experiments show that the initial failure mode of the slab is cracking, occurred in the surface of the slab. In effect, these cracks partly result from the fact that the tensile stress exceeds the tensile strength σ_t . Therefore, if the tensile stress σ_{up} (or σ_{down}) in the surface of the middle of the beam elements exceeds σ_t , the crack will occur.

(3) The dam-water coupling vibration

In the case of water storage, the boundary element method is employed in this paper to assess the added mass matrix produced by the seismic water pressure.

Selection of Parameters for Analyses According to the experiments of model dams and referring to the data presented in the literature(Ref.1,2), some necessary parameters which are given in Table 3 are specified.

The input motion used in the numerical analysis is the same as the motion exciting the shaking table in the experiment, i.e., $a(t) = t \cdot \sin(2\pi ft)g/450$, in which, the forced frequency $f=20\text{Hz}$, the duration of each step $\Delta t=1/16f$, the large duration used in the iteration modelling the nonlinearity of soil is selected three times of period, $3/f$.

Analytical Results The model dams are represented by 90 two-dimensional isoparametric elements(embankment), 12 beam elements(facing slab), and 12 joint elements arranged along the contact surface between the facing slab and the embankment.

As an example, the distributions of accelerations in the embankment and the stresses in the slab at the beginning of the initial sliding and cracking of slab with two different cases of reservoir level are given in Fig.9 and Fig.10. The shadow zones marked in the figures stand for the failing soil mass. The initial failure of model dams always occurs near the crest, which is independent of the reservoir water level. It should be stressed that during earthquakes, significant increases of stresses on the upper portion of the slab, due to failing of soil mass near the crest, yield the initiation of cracking on the slab in the corresponding position. The reservoir water makes the actual position of cracks move up. These computational results are in good agreement with the model experiments.

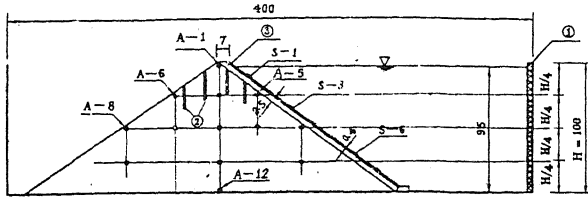
CONCLUSIONS

On the basis of above experimental and computational results, the following conclusions can be drawn.

1. For the transverse vibration, the natural frequencies of faced rockfill dams slightly increase with respect to the homogeneous rockfill dams. This influence decreases with the dam height. It can be neglected due to the small value of E_f/E_d for the high faced rockfill dams. Subsequently, the vibration characteristics of these dams can be estimated by the conventional procedure without significant errors.
2. It seems that frequencies of the faced rockfill dams are, on the whole, independent of the level of reservoir water.
3. The contributions of the facing slab to the vibration shapes mainly lie in the higher modes, especially for the transverse vibration.
4. The failure of faced rockfill dams occurs near the crest of the downstream slope. It takes the form of the shallow-seated slip. The upstream slope has a rather high stability due to the facing slab.
5. Under strong earthquakes, the failing of the soil mass near the crest, including loosening, sliding and subsiding, leads to the loss of supports of the soil on the slab, the significant increases of stresses should be responsible for the fracture occurred in the upper of the slab. Moreover, the actual position of the fracture is intimately related to the level of reservoir water.

REFERENCES

1. Kenzo Toki, and Fusanori Miura, Non-Linear Seismic Response Analysis of Soil-Structure Interaction System, Proceedings of the Japan Society of Civil Engineers, (1982).
2. Fumio Tatsuoka, Xianjing Kong, and Tej B.S. Prodhon, Dynamic Deformation Properties of Sand at Extremely Low Pressures, Proceeding of the Seventh Japan Earthquake Engineering Symposium, (1986).



① Sponge ② Colour Sand ③ Slab • Accelerator - Strain Gauge
Fig.1 Cross Section of Model Dam

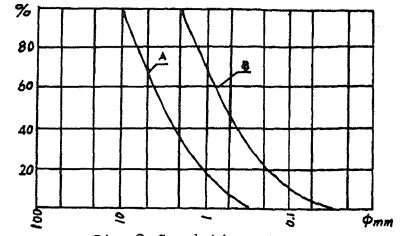


Fig.2 Gradation Curve

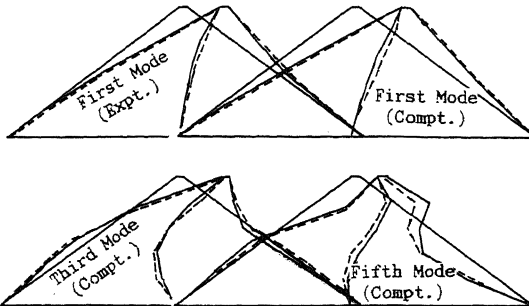


Fig.4

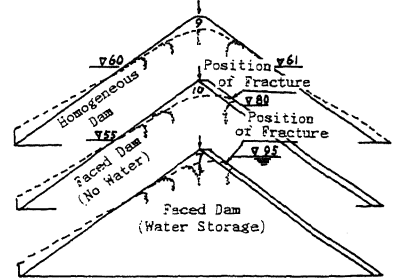


Fig.5 Failure States of the Model Dams

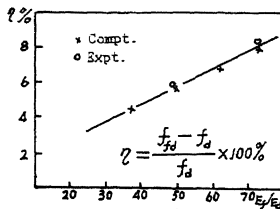


Fig.3

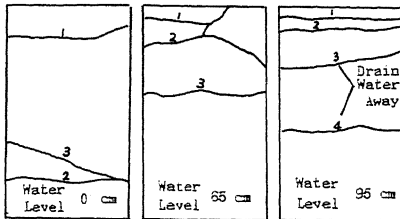


Fig.6 Occurrence Sequence of Fracture

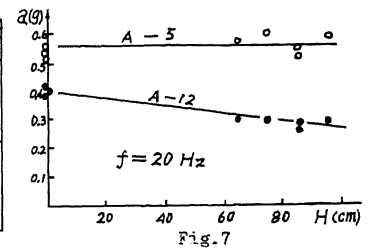


Fig.7

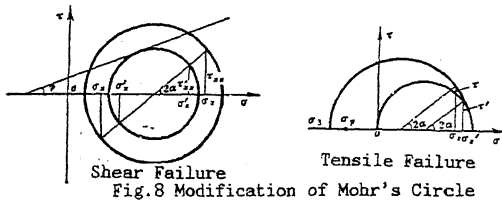


Fig.8 Modification of Mohr's Circle

Table 1 Experimental and Computational Frequencies (Hz)

Mode Number	Homogeneous Dam		Faced Dam With Gypsum		Faced Dam With plexiglass	
	Expt.	Compt.	Expt.	Compt.	Expt.	Compt.
1	43	42.86	45.5	45.32	46.5	46.36
2		71.97		72.34		72.61
3		77.63		82.19		83.34
4		96.37		97.72		97.98
5		104.34		108.95		109.60
6		109.82		110.04		110.47

Table 3 Material Properties of Model dam

Facing Slab	Tensile Strength $\sigma_t = 2.0 \text{ kgf/cm}^2$
Slab	Dynamic Modulus $E_d = 24000 \text{ kgf/cm}^2$
Joint	Shear const $K_s = 10^6 \text{ tf/m}^2$
Element	Normal const $K_n = 2 \times 10^6 \text{ tf/m}^2$ Cohesion
	Internal Friction Angle $\phi = 50^\circ$, $C = 0$
Dam Shell	$G_{max} = 658 \sigma_m^{0.33} \text{ (kgf/cm}^2\text{)}$ Cohesion
	Internal Friction Angle $\phi = 55^\circ$, $C = 0$
Filter	

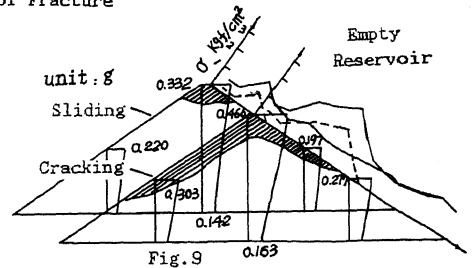


Fig.9

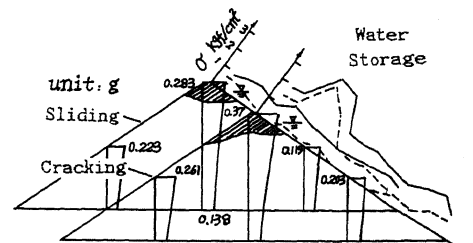


Fig.10

Table 2 Relationship Between Subsiding and Position of Fracture with Water Level

Measured Parameter	Water Levels (cm)				
	0	65	75	85	95
Subsiding Depth	11.6	10.8	7.0	8.5	8.25
Position of Fracture	27.6	35.5	11.5	13.75	8.7